European Journal of Mechanics / A Solids 100 (2023) 105010

Contents lists available at ScienceDirect

European Journal of Mechanics / A Solids

journal homepage: www.elsevier.com/locate/ejmsol

Racing bicycle tyres – Influence on mechanical characteristics of internal pressure, vertical force, speed and temperature

G. Dell'Orto [a,*], F.M. Ballo [a], G. Mastinu [a], M. Gobbi [a], G. Magnani [b]

[a] Department of Mechanical Engineering, Politecnico di Milano, Via La Masa 1, 20156, Milan, Italy
[b] Department of Electronics, Information and Bioengineering (DEIB), Politecnico di Milano, Via Ponzio 34/5, 20133, Milan, Italy

ARTICLE INFO

Keywords:
Flat track
Drum
Tyre drop
Contact patch
Inflation pressure
Temperature
Speed

ABSTRACT

The paper describes how internal pressure, vertical force, speed and rolling surface temperature may affect the mechanical characteristics of a road racing bicycle tyre. The results were obtained from an experimental test campaign performed with VeTyT, a test-rig specifically designed for measuring the mechanical characteristics of bicycle tyres.

The static deflection of tyre for different inflation pressures and vertical loads was measured to determine the static tyre vertical stiffness. Results for tyre rolling on flat track or on a drum were compared. Dynamic analyses were focused on evaluating the effect of inflation pressure and vertical load, for two rims featured by different lateral stiffness. Then, the respective effects of speed and of temperature of the rolling surface on the lateral force were considered.

Stiffer rims can ensure higher values of cornering stiffness. In addition, higher inflation pressure is recommended only for heavy vertical loads. For low vertical loads, too inflated tyre results to be less performant, i.e. to show lower values of cornering stiffness. The speed can affect the mechanical characteristics of bicycle tyres mainly for slip angles less than 1.5°, while the temperature of the rolling surface is the most affecting parameter for slip angles larger than 3°.

1. Introduction

After Covid-19 pandemia, many people rediscovered the pleasure of cycling (Brooks et al., 2021). Cycling is a healthy activity, and it is expected to follow an increasing trend in the upcoming years (Corwin et al., 2020), (Deloitte's, 2020). To manage and facilitate the transitions through new ways of mobility, it is essential to ensure ride comfort and safety. Some researchers have already dealt with new layouts of road intersections "cycling-friendly" (Yang et al., 2019), but very few studies are focused on bicycle design (Corno et al., 2021). Mathematical models are required to understand bicycle dynamics, but they need to be implemented with realistic tyre parameters (Kresie et al., 2017), (Hess et al., 2012). Tyres are very important to ensure safer vehicle handling, since their mechanical characteristics can strongly affect vehicle dynamics (Mastinu and Ploechl, 2014) (Evangelou, 2003), (Pacejka, 2006) This statement is even more important for two wheeled vehicles, such as motorcycles and bicycles, featured by a relatively small contact patch between tyre and road (Doria and Roa Melo, 2018) (Takács et al., 2009).

As well as motorcycle tyres, bicycle tyres are featured by a toroidal cross-section of the carcass (Sharp, 1971), (Sharp, 1993), but they are completely different in construction and usage, being designed for much smaller loads. In (Doria et al., 2013), bicycle tyres were tested for different working conditions. A decrease in lateral force was recorded with a decrease in inflation pressure. This phenomenon was explained considering a reduced lateral stiffness when the inflation pressure decreased. In addition, it was noted that an increase in vertical load resulted in a decreased normalized lateral force. Similar tests were performed in (Maier et al., 2018), where a set of mountain bike tyres was tested for different vertical loads and inflation pressures. It was found an increase in cornering stiffness with the pressure. Above a certain pressure, all the tyres showed a constant value of cornering stiffness. The latter is useful for modeling, since it may affect vehicle dynamics (Bulsink et al., 2015).

It is important to understand how different parameters may affect tyre characteristics. Despite this, very few studies are presented on this topic. Bicycle-rider models often lack information on tyres (Moore, 2012). Shimmy (or "wobble") is a dynamic instability which may affect bicycles (especially road racing bicycles, running at high speed). Some

* Corresponding author. .
E-mail address: gabriele.dellorto@polimi.it (G. Dell'Orto).

https://doi.org/10.1016/j.euromechsol.2023.105010
Received 2 January 2023; Received in revised form 18 April 2023; Accepted 24 April 2023
Available online 28 April 2023

mathematical models have been presented in the past, trying to understand the phenomenon. Nonetheless, the researchers pointed out the necessity to have measured tyre characteristics to refine the models (Klinger et al., 2014) (Tomiati et al., 2017). This paper tries to close the gap, providing measurements of the mechanical characteristics of road racing bicycle tyre to some extent. Both static and dynamic analysis are carried out on a 26 mm wide road racing bicycle tyre, mounted on aluminum commercial rim and on high-stiffness laboratory rim in order to investigate the effect of rim stiffness on lateral characteristics. The static tests involve tyre not rolling on the contact surface, therefore tyre deflection and contact patch measurements varying inflation pressure and vertical load (Section 1 and Section 2). Dynamic contact patches are still hard to measure on such test-rig, as a proper test bench should be implemented to the purpose (Swami et al., 2021). The dynamic tests were performed with tyre rolling on the contact surface to measure the lateral force F_y and the self-aligning torque M_z (Section 3). Tests were performed both on flat track and on a 2.6 m diameter drum (known as "RuotaVia" (Mastinu et al., 2002)). The effect of inflation pressure, vertical load and rim stiffness was evaluated on lateral force and cornering stiffness. After that, the focus is devoted to the effect of the speed on the variation of lateral force. Finally, it is studied how the rolling surface temperature can affect the lateral force F_y.

1.1. Methods

Tests are performed with VeTyT, a testing machine specifically designed for bicycle tyres (Dell'Orto et al., 2022a) (Dell'Orto et al., 2022b). The measuring procedure has been certified in accordance with the standard UNI EN ISO 9001.

The aluminum frame carries a bicycle tyre on a flat track or on the top of a drum. The whole chassis can be tilted to set the camber angle in the range ±25°, while the slip angle α can be adjusted rotating the steering shaft. The vertical load acting on the wheel can be varied adding masses on the frame. It can measure lateral force, self-aligning torque and vertical force. The complete assembly of the test-rig is shown in Fig. 1.

Tests were performed on a road racing bicycle tyre (26 mm wide), for different inflation pressures, ranging from 3.5 to 7.5 bar, declared by manufacturer as upper limit. The value of 3.5 bar was chosen to simulate a wrong inflation pressure or a flat tyre after punching. The tyre was mounted with inner tube.

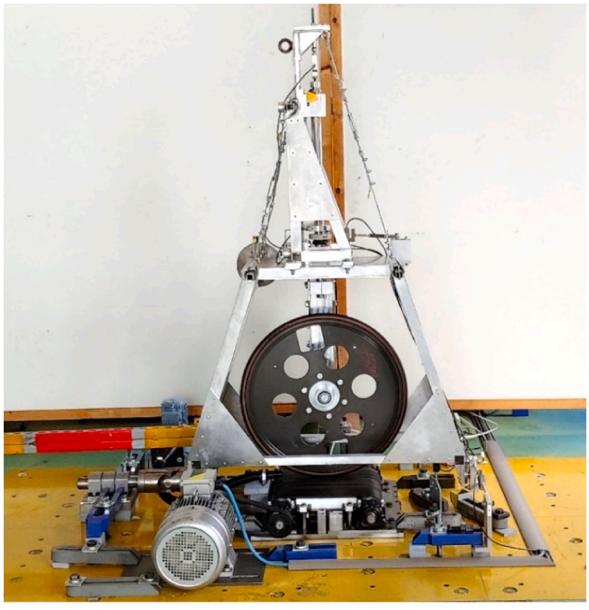

Fig. 1. VeTyT test-rig at Politecnico di Milano. In this picture, the frame carries a high-stiffness laboratory rim running on flat track (Dell'Orto et al., 2022a).

Three different vertical loads were tested: 340 N, 400 N and 490 N. The values were chosen being consistent with the mass of common riders and bicycles, as reported in Table 1.

The load ratio represents the load distribution front/rear wheel of the bicycle. The value 50/50 is compatible with road racing bicycles (Carahalios, 2015), while the bicycle mass of 10 kg is feasible for a carbon frame bicycle equipped with two water bottles and pedals.

2. Static analysis

2.1. Static tyre deflection

Static tyre deflection (also known as tyre drop) corresponds to the tyre deflection due to the application of a vertical load (Berto, 2006) (SAE International, 2019). It is a quantity of interest since it is related to the extension of contact patch and can be assumed as a reference for setting the optimal tyre inflation pressure (Heine, 2006). From the knowledge of static tyre deflection, the normal stiffness can also be derived.

The static tyre deflection (tyre drop) was measured both on a flat track and on the RuotaVia drum (Mastinu et al., 2002). Tyre was mounted on aluminum commercial rim and tested for different inflation pressures and vertical loads.

2.1.1. Methods

VeTyT was used for the measurements of the static tyre deflection. A 26 mm wide road racing bicycletyre was mounted with inner tube on an aluminum commercial rim. A proper gauge was employed to measure the height. It was placed on the base of the rolling surface (flat track or RuotaVia drum, respectively), so that its probe was in contact with the rim (set-up depicted in Fig. 2). After the application of vertical load, the difference between the undeformed and deformed height of the tyre was recorded. Three different vertical loads were applied (340 N, 400 N and 490 N), for inflation pressures ranging from 3.5 bar to 7.5 bar. All the experiments were led in laboratory at room temperature (23 ± 4 °C), and tests were repeated three times and averaged.

2.1.2. Results

In Fig. 3, the static tyre deflection is depicted as function of vertical load for different inflation pressure, for the tests on the flat track. The relationship between tyre drop and vertical load results to be almost linear for all the tested inflation pressures. The same can be concluded for the RuotaVia drum (Fig. 4), since the trend is linearly increasing with the vertical load. As expected, the increase of vertical load causes a larger deflection of the tyre, independently of the inflation pressure. On the RuotaVia drum (Fig. 4), the maximum values achieved are larger than those measured on the flat track, for all the tested inflation pressure values. This can be explained considering the shape of the contact patch tyre/rolling surface. The curvature of RuotaVia drum affects the contact patch length, acting on a smaller contact area.

It can be assumed that the contact patch length decreases at increasing curvature of the rolling surface ($\frac{1}{R}$, where R stands for RuotaVia radius) (Phromjan and Suvanjumrat, 2020). When the radius of drum is significantly smaller than the radius of the tyre, the contact patch could be schematized as a single point (Fig. 7). The area of the contact patch decreases at increasing the curvature of the contact surface. According to this statement, a smaller portion of the tyre should

Table 1
Rider/bicycle mass, load distribution front/rear, tyre vertical load.

Rider mass	Bicycle mass	Load ratio	Vertical load on tyre
58 kg	10 kg	50/50	≈340 N
70 kg	10 kg	50/50	≈400 N
88 kg	10 kg	50/50	≈490 N

Fig. 2. Set-up for measuring the static tyre deflection with VeTyT, here depicted for RuotaVia drum.

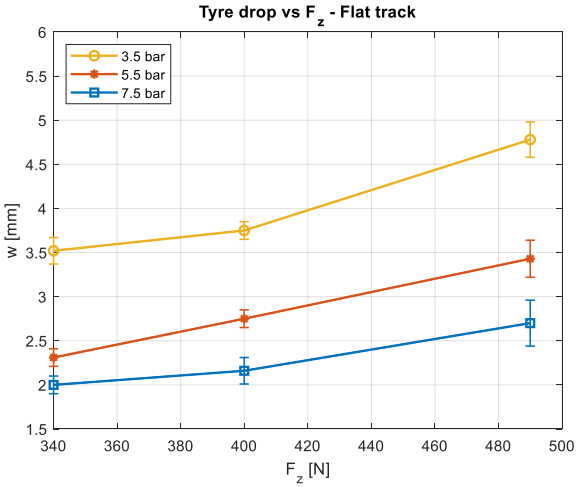

Fig. 3. Tyre drop as function of vertical load, for different inflation pressure (see legenda), here depicted for flat track. A 26 mm wide tyre was tested.

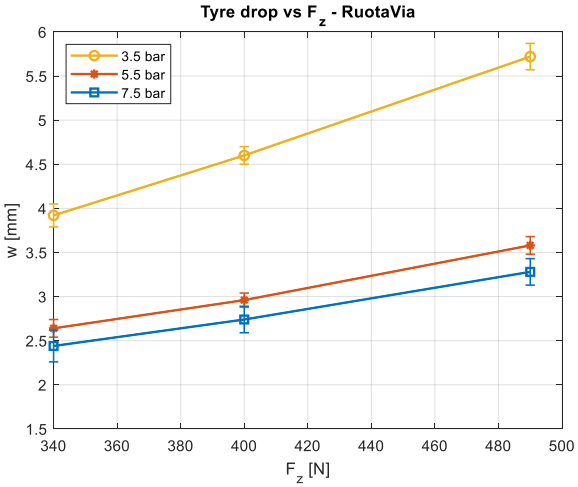

Fig. 4. Tyre drop as function of vertical load, for different inflation pressure (see legenda), here depicted for RuotaVia. A 26 mm wide tyre was tested.

sustain the vertical load, so that a higher value of tyre drop is expected. Therefore, a smaller value of vertical stiffness for the measurements performed on RuotaVia drum is expected (see Table 1).

On average the values of static deflection of tyre measured on RuotaVia are 18% larger than those measured on flat track (see Table 2).

Concerning the tyre drop as function of inflation pressure, the trend is linearly decreasing at increasing the inflation pressure, for tests on the flat track (Fig. 5). As expected, larger pressures mean higher load capacity, so less static deflection at constant vertical load. The behavior is slightly different for the RuotaVia drum (Fig. 6). As already mentioned for Figs. 3 and 4, the deflection values for the RuotaVia drum are larger than those recorded for the flat track.

The values of static deflection of tyre tested on flat track and on RuotaVia drum are summarized in Table 2. The results on RuotaVia drum and on flat track are evaluated in the last column. As already mentioned, an average variation of 18% can be appreciated, being the values on RuotaVia drum always larger than those on flat track.

Comparing the results, it is clear the difference in magnitude for the tests on the RuotaVia drumand on the flat track. All the results on flat track are smaller than those on RuotaVia drum, for all the considered vertical loads and inflation pressures.

The evaluation of vertical stiffness was then carried out linearly interpolating the experimental data. The results are shown in Figs. 8 and 9. The vertical stiffness corresponds to the slope of the curves, as reported in the legenda of the figures below. The vertical stiffness increases as inflation pressures increases, both for RuotaVia and flat track.

The comparison of the results is summarized in Table 3. Vertical stiffness measured on the RuotaVia drum is always less than that on the flat track. On average, a reduction of 14% was found. A reduction in contact area due to the shape of contact patch tyre/drum may be the main cause of this difference, as explained above.

2.2. *Tyre contact patch*

An analysis to evaluate the area and the shape of contact patch on

Table 2
Measurement of tyre drop for flat track and RuotaVia drum (2.6 m diameter), and the % variation of results. The values were obtained for a 26 mm wide tyre.

Pressure [bar]	Vertical Load [N]	Tyre drop w [mm] – Flat track	Tyre drop w [mm] – RuotaVia drum	% Variation RuotaVia drum VS Flat track
3.5	340	3.52	3.92	11%
	400	3.75	4.60	22%
	490	4.78	5.72	20%
5.5	340	2.31	2.64	14%
	400	2.75	2.96	7%
	490	3.43	3.58	4%
7.5	340	2.00	2.44	22%
	400	2.16	2.74	27%
	490	2.70	3.28	21%

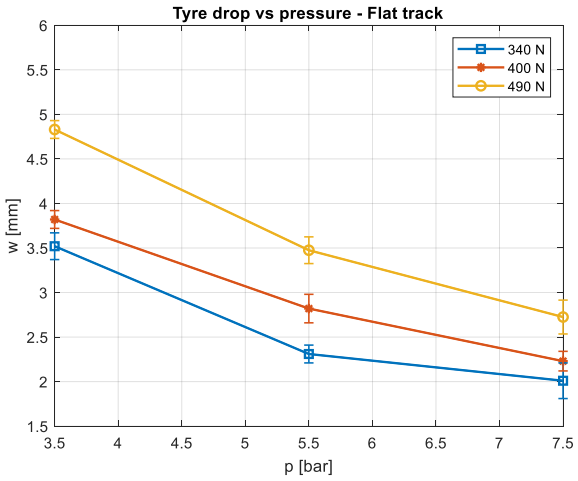

Fig. 5. Tyre drop as function of inflation pressure, for different vertical loads (see legenda), here depicted for flat track (26 mm wide tyre).

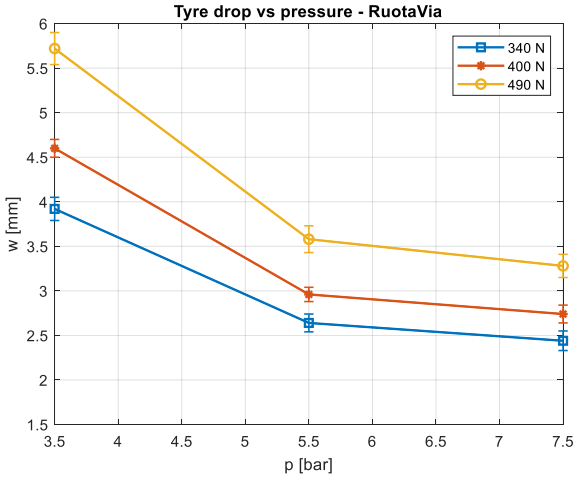

Fig. 6. Tyre drop as function of inflation pressure, for different vertical loads (see legenda), here depicted for RuotaVia. A 26 mm wide tyre was tested.

RuotaVia drum or on flat track was carried out. Contact patches were experimentally determined both using pressure sensitive film and chalk dust.

A sensitive pressure film was placed under the tyre, so as to impress on it the shape of the contact patch (Fig. 11). Then, the film was scanned and post-processed through an ad hoc MATLAB® script. It was possible to measure the total area and the pressure distribution. Tests were performed for different inflation pressures and vertical loads.

For the sake of accuracy, measurements were then repeated covering the tyre with chalk powder. A black cardboard was placed under the contact surface (Fig. 10). As first approximation, the contact patches were assumed to be elliptical. The lengths of major and minor axis (we refer as a and b, respectively) were measured through a gauge. The area

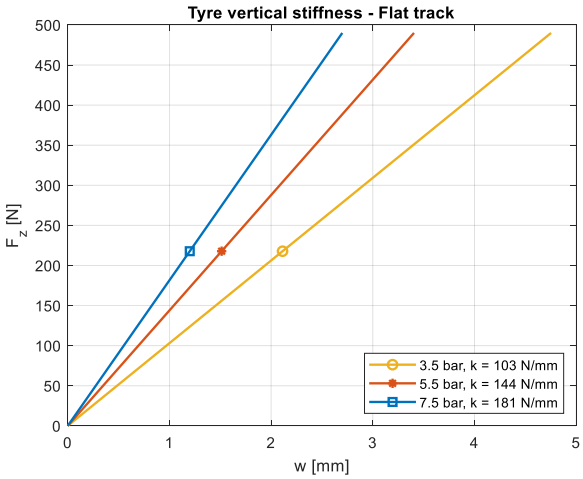

Fig. 8. Tyre drop as function of vertical loads, for different inflation pressure. Results obtained on flat track.

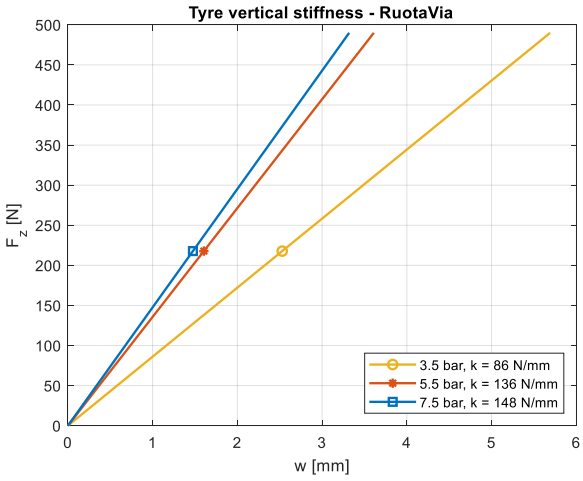

Fig. 9. Tyre drop as function of vertical loads, for different inflation pressure. Results obtained on RuotaVia drum.

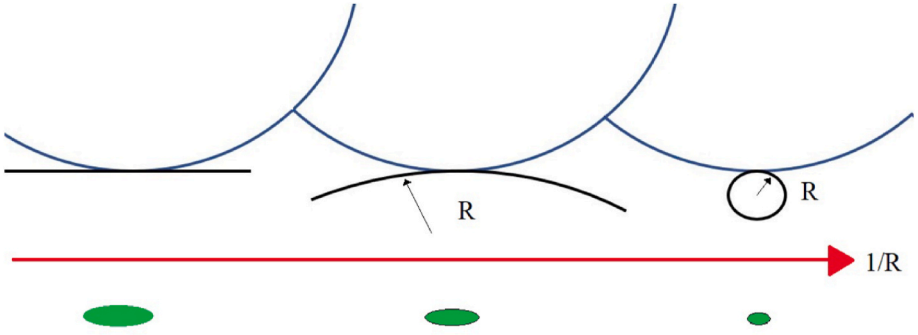

Fig. 7. Contact patch variation at increasing the curvature of the rolling surface. In green, the expected contact patch, in blue the tyre, in black the rolling surface. At left, the case of R equal to ∞, i.e. the flat track. At right, the case with R close to zero, so curvature very large. (For interpretation of the references to color in this figure legend, the reader is referred to the Web version of this article.)

Table 3
Vertical stiffness, comparison for results from RuotaVia and flat track, tested for different inflation pressures.

Pressure [bar]	$\mathbf{K_z}$ [N/mm] – Flat track	$\mathbf{K_z}$ [N/mm] – RuotaVia	% Variation RuotaVia VS Flat track
3.5	103.1	86.1	−16%
5.5	143.9	135.7	−6%
7.5	181.5	147.6	−18%

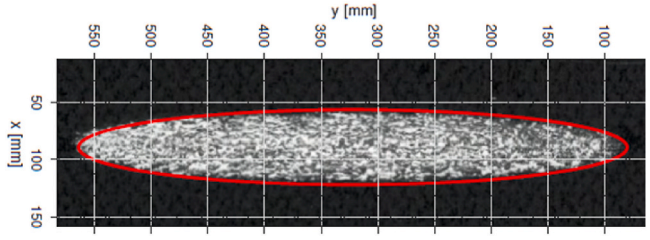

Fig. 10. Contact patch obtained with chalk powder and a black cardboard, on flat track. In red, the ellipse approximation of the contact patch. (For interpretation of the references to color in this figure legend, the reader is referred to the Web version of this article.)

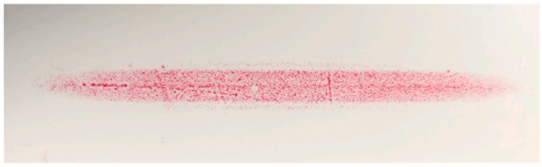

Fig. 11. Contact patch obtained with pressure sensitive film.

was calculated according to (2.1).

$$\text{Area} = a\, b\, \pi$$

Contact patches were then scanned and processed by the software IMAGEJ®, usually employed in the field of microbiology (Schneider et al., 2012) (Abràmoff et al., 2004). The effectiveness of considering contact patch as an ellipse was confirmed, with a difference less than 5% on the total area measured with (2.1). Results were also confirmed for the pressure sensitive film.

The contact patches on flat track are on average 12% larger than those on RuotaVia drum. The difference is related to the curvature of the RuotaVia drum, which affects the shape of the contact. It mainly changes the length of contact patch, with a reduction from RuotaVia drum to flat track in the order of 10%. Increasing the vertical load, the difference in contact patch area decreases.

3. Dynamic measurements

3.1. Combined effect of inflation pressure and vertical load on cornering stiffness

The dynamic tests on bicycle tyres were performed on flat track, with tyre mounted both on a commercial rim and on a high-stiffness rim. Flat track surface was covered by sand of controlled granulometry (1.2 mm), to simulate the road surface.

The cornering stiffness can be evaluated according to (3.1).

$$C_{F_y} = \frac{\delta F_y}{\delta \alpha}\Big|_{\alpha=0} \tag{3.1}$$

Once measured the lateral force F_y as function of slip angle α, C_{F_y} can be derived. The values of cornering stiffness evaluated according to (3.1) are depicted in Figs. 12 and 13 for standard aluminum rim and high-stiffness laboratory rim, respectively. The values were then interpolated with high-order polynomial, to understand the relationship between cornering stiffness and vertical load applied to the tyre.

The value of C_{F_y} largely changes with inflation pressure. As depicted in Fig. 12, the values for the inflation pressure of 7.5 bar are higher than those for inflation pressure 3.5 bar. The peak of cornering stiffness for inflation pressure 7.5 bar corresponds to the maximum tested vertical load of 490 N. The trend is not confirmed for lower inflation pressures, where the peak of cornering stiffness can be found for lower vertical load. Similar trend was also found for tyre mounted on high-stiffness rim (Fig. 13), which can strongly affect the tyre performance. The highest values of cornering stiffness are obtained with the stiffest rim (Fig. 13). The rim used for these tests is approximately five times stiffer than a standard aluminum rim. The results of cornering stiffness for the tested rims are summarized in Table 4. Independently on the inflation pressure or on vertical load, the value of C_{F_y} is on average 13% higher for the high-stiffness rim.

The effect of inflation pressure is also crucial for ensuring good performance. Both for standard and high-stiffness rim, an increase in inflation pressure means an increase in cornering stiffness. This trend was found only for vertical loads larger than a certain threshold equal to 400 N. Below that value, a tyre less inflated seems to perform better. This can be understood thinking about the need of adjusting pressure according to vertical load (Heine, 2006). A too inflated tyre shows a small contact patch if the vertical load is not sufficient to push the tyre on the road. Another experimental campaign was carried out on a different model of 26 mm wide road racing bicycle tyre, tested on flat track and mounted on standard rim to validate the hypothesis. Tests were performed with many different inflation pressure and vertical loads (Fig. 14).

Looking at Fig. 14, we can notice that for a vertical load close to 250 N a lower inflation pressure is required to ensure higher values of cornering stiffness. On the contrary, higher inflation pressures result in high cornering stiffness for large vertical loads (clearly visible for vertical load larger than 600 N).

3.2. Effect of the speed

The effect of the rolling speed on the lateral force of bicycle tyre was evaluated. Tests were performed on the flat track by varying the speed of the rolling surface between 4 km/h up to 23 km/h.

A 26 mm wide road racing bicycle tyre was tested for a vertical load

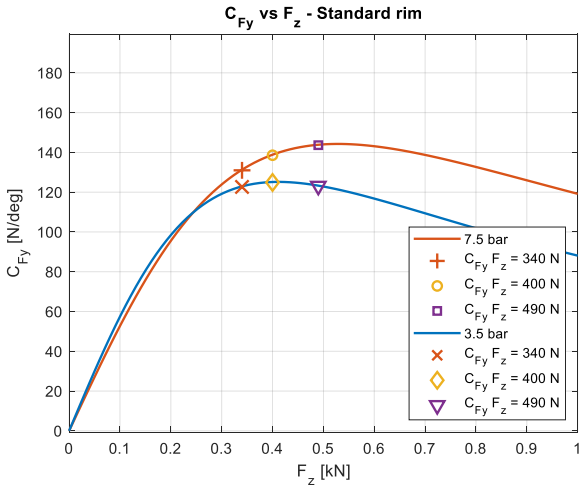

Fig. 12. Cornering stiffness C_{F_y} as function of the vertical load F_z. The red curve is for inflation pressure of 7.5 bar, the blue one is for 3.5 bar. Tyre was tested on flat track, mounted on standard commercial rim. (For interpretation of the references to color in this figure legend, the reader is referred to the Web version of this article.)

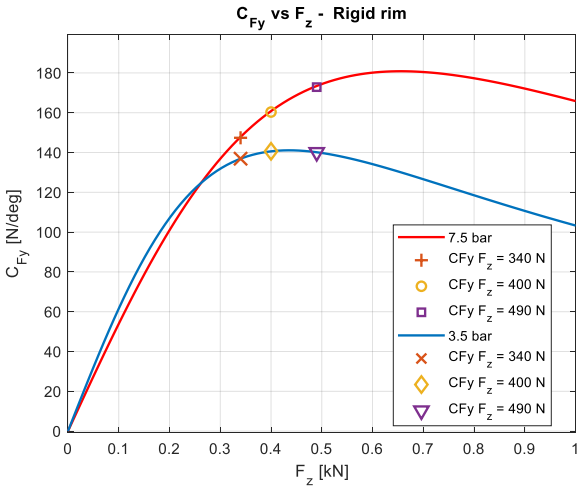

Fig. 13. Cornering stiffness C_{F_y} as function of the vertical load F_z. The red curve is for inflation pressure of 7.5 bar, the blue one is for 3.5 bar. Tyre was tested on flat track, mounted on high-stiffness rim. (For interpretation of the references to color in this figure legend, the reader is referred to the Web version of this article.)

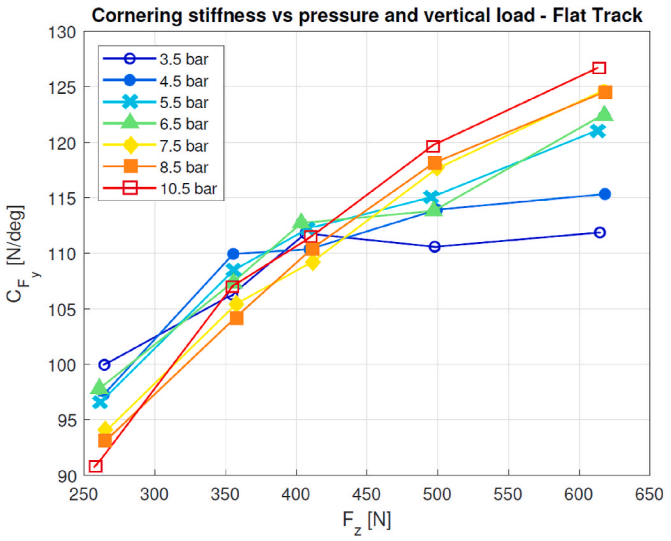

Fig. 14. Cornering stiffness for a 26 mm road racing bicycle tyre as function of vertical load. The curves of different colors correspond to different inflation pressures. Tests were carried out on flat track. (For interpretation of the references to color in this figure legend, the reader is referred to the Web version of this article.)

Table 4
Cornering stiffness values for tyre mounted on standard aluminum rim and high-stiffness rim, for different inflation pressures and vertical loads. The percentage of variation of the cornering stiffness for different rims (standard or high-stiffness one) is reported in the last column.

p [bar]	F_z [N]	C_{F_y} [N/deg] (U = 1.5%) Standard rim	C_{F_y} [N/deg] (U = 1.5%) High-stiffness rim	Variation High-stiffness rim VS Standard rim
3.5	**340**	122.6	136.9	+12%
	400	124.9	140.6	+12%
	490	123.1	140.1	+14%
5.5	**340**	131.1	145.3	+11%
	400	137.7	155.2	+13%
	490	141.2	163.2	+16%
7.5	**340**	131.0	147.4	+13%
	400	138.6	160.3	+16%
	490	143.7	172.9	+20%

equal to 400 N and inflation pressure of 7.5 bar. The results for lateral force are depicted in a carpet plot for positive slip angles only (Fig. 15). This allows to appreciate the variations of lateral force F_y increasing the speed of the rolling surface.

For slip angles close to zero, the lateral force slightly increases linearly with the speed.

Considering slip angles higher than 2°, the trend of variation is no more linear. Lateral force achieves a maximum for the speed equal to 16 km/h, then it slightly decreases. This phenomenon may be due to increase of the temperature of the rolling surface. Lateral force is expected to linearly increase with the speed, but for high slip angles the heat generated by the friction between the flat belt and the supporting surface increases as well. The effect of the temperature generates a decrease in the measured lateral force, as discussed in the next section.

Table 5 summarizes the percentage of variation of the measured lateral force with respect to the lowest speed tested (4 km/h), taken as reference. It can be noticed that the lateral force increases as the speed of the rolling surface increases, almost linearly for slip angles less than 2°. The trend changes for high slip angles, for which the effect of the temperature may affect the measurements (Dell'Orto and Mastinu, 2022).

The values reported in Table 5 demonstrate that the effect of the speed variation is almost negligible for slip angles larger than 2°. On the contrary, the effect of the temperature must be considered as detrimental for the measurements for high speeds of the rolling surface and high slip angles. VeTyT has been recently updated for compensating this effect. A cooling system was designed and implemented to remove the heat close to the contact patch tyre/flat track (Dell'Orto et al., 2022a).

3.3. Effect of the temperature

In this Section, the effect of temperature variation on the lateral force of bicycle tyre is studied. A 26 mm wide road racing bicycle tyre was used for the tests, mounted on high-stiffness laboratory rim. Specifically, the main parameter of interest is the temperature of the rolling surface. This is simpler and more accurate to be measured if compared to the tyre external surface (Farroni et al., 2020) (Farroni et al., 2014). In addition, it may be the independent variable of interest for riders and cycling professional teams. The vertical load was set to 400 N and the inflation pressure to 7.5 bar.

The lateral force was measured and plotted as function of the temperature of the flat track. The latter was measured with an infrared thermometer and a thermocamera in the area close to the contact patch. In Fig. 16, the lateral force is reported as function of the recorded temperature. The slip angle was set to 3.3°.

It is possible to note the remarkable correlation between the decrease of the measured values and the increase of temperature. While the temperature increases from 32 °C to 50 °C, the lateral force decreases of 11%, showing a quadratic decreasing trend. Additional tests were performed setting the slip angle at 5°. The results are collected in Fig. 17. We can note that data follow a quadratic decreasing trend, as well as results for slip angle equal to 3.3°. Increasing the temperature, the lateral force decreases 16% for a variation in temperature of 40 °C. The important role played by the temperature is even more evident for large slip angles.

The decreasing trend with the increase of temperature is confirmed for slip angles $|\alpha| > 3°$. Repeating the test for slip angle equal to 1°, the results are completely different, as shown in Figure Fig. 18. The variability is much smaller and limited to less than 1% for lateral force.

Observing Fig. 18, values are almost constant and can be interpolated by a straight line (angular coefficient equal to 0.01). Repeating tests for other slip angles $|\alpha| < 3°$ a clear trend cannot be distinguished, but variability remains however lower than 2% for lateral force.

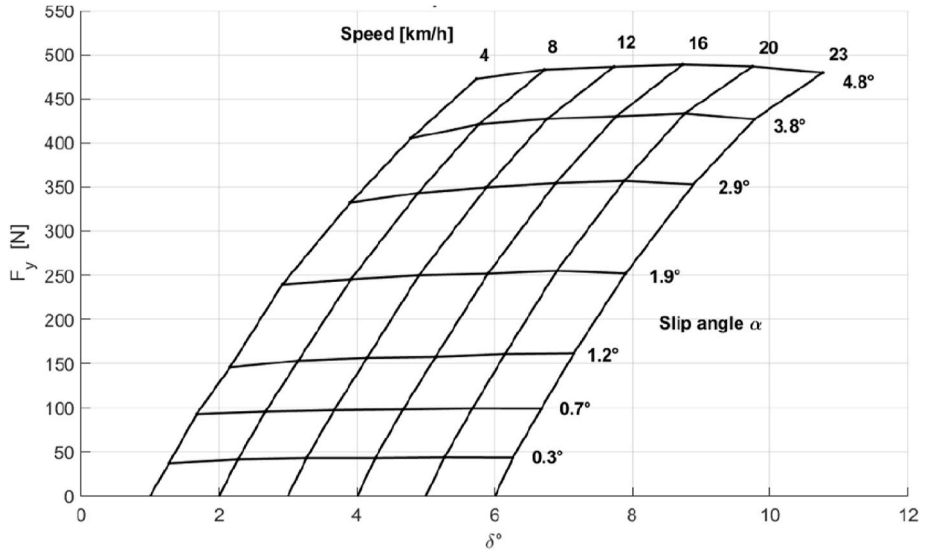

Fig. 15. Influence of the speed of rolling surface on the lateral force. In the upper part of the plot, the values of speed are reported. At right, values of slip angles are shown.

Table 5
Percentage variation of the lateral force with respect to the values measured at speed 4 km/h, up to 23 km/h. A 26 mm wide tyre was tested.

Δ_{F_y} %		Speed [km /h]					
		4	**8**	**12**	**16**	**20**	**23**
Speed [km /h]	**0.3**	0	12	16	15	17	16
	0.7	0	3	5	6	7	7
	1.2	0	5	8	8	10	11
	1.9	0	2	4	5	6	5
	2.9	0	3	5	7	7	6
	3.8	0	4	5	6	7	5
	4.8	0	2	3	3	3	1

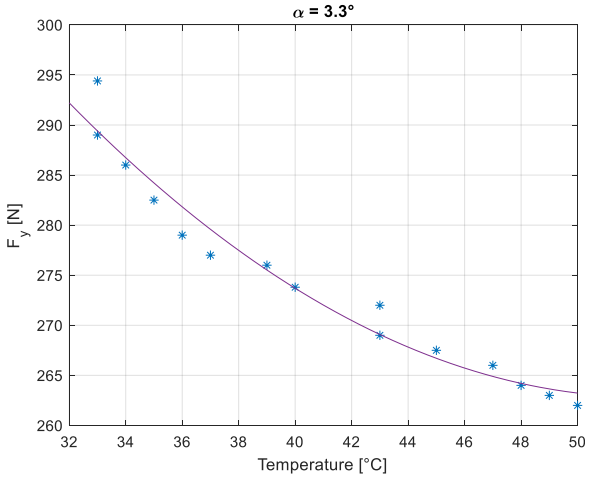

Fig. 16. Lateral force as function of recorded temperature of flat track, for slip angle equal to 3.3°. In violet the data interpolating line (second order polynomial interpolation). (For interpretation of the references to color in this figure legend, the reader is referred to the Web version of this article.)

These effects could be relevant considering paved roads during summer, when the presence of shaded corners may cause a sudden increase/decrease in road temperature, thus changing the bicycle handling. This is strictly connected to bicycle dynamics, and it could be relevant for the occurrence of sudden and dangerous dynamic instabilities (Tomiati et al., 2017), (Tomiati et al., 2019).

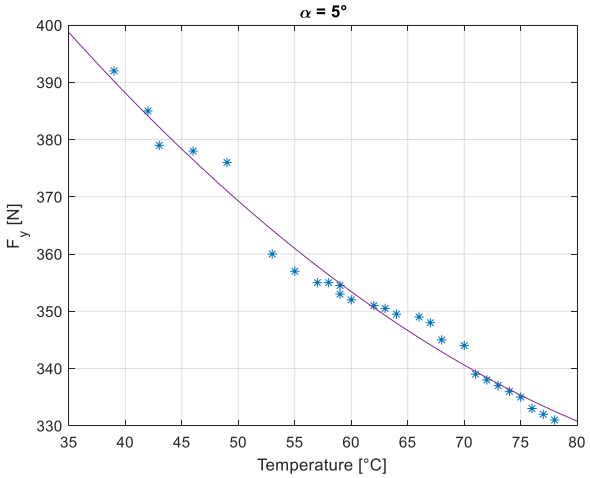

Fig. 17. Lateral force as function of recorded temperature of flat track, for slip angle of 5°. In violet the data interpolating line (second order polynomial interpolation). (For interpretation of the references to color in this figure legend, the reader is referred to the Web version of this article.)

4. Conclusions

In the paper, the results of some external parameters on the mechanical characteristics of a 26 mm road racing bicycle are presented. Both static and dynamic tests were performed.

Specifically, it was considered the effect of the inflation pressure, vertical load, type of rolling surface (flat track or drum), stiffness of the rim, speed and temperature.

Vertical stiffness was statically measured for different vertical loads and inflation pressure, both on a flat track and the RuotaVia drum (drum of 2.6 m of diameter). Static tyre vertical stiffness is defined as the ratio between the applied load and the static deflection of the tyre. Static deflection is important since manufacturers provide recommended inflation pressure on the basis of the static deflection, also known as "tyre drop".

Summarizing the results obtained from tests, we have.

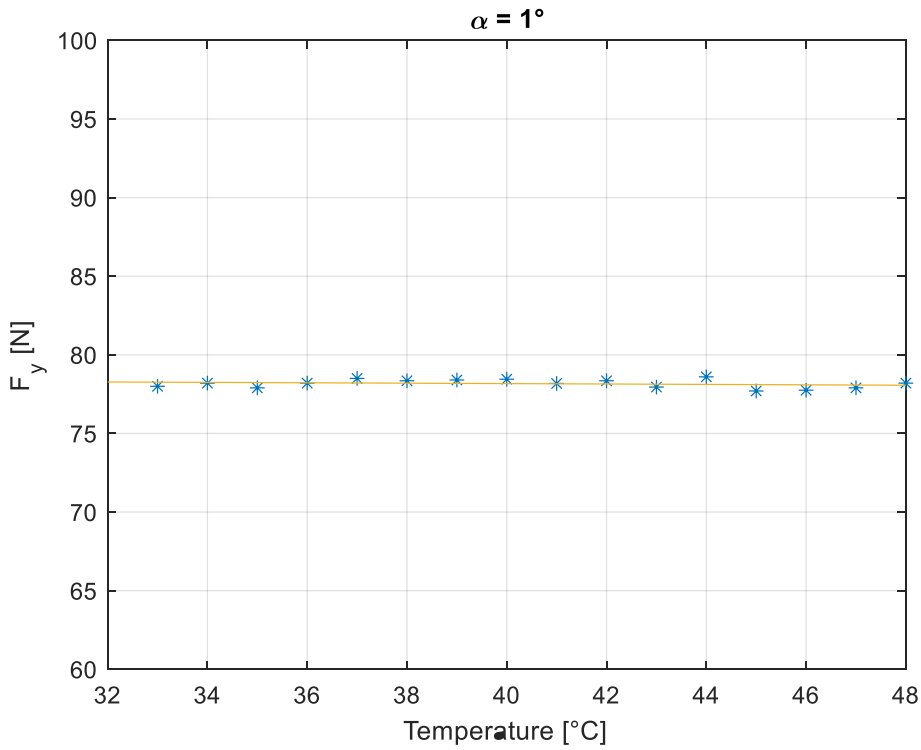

Fig. 18. Lateral force as function of recorded temperature of flat track, for slip angle equal to 1°. Data can be interpolated by a straight line of.

- The static deflection on RuotaVia was found to be on average 18% higher than one measured on flat track, for all vertical loads and inflation pressures tested. The curvature of RuotaVia drum may affect the contact patch length, acting as a punch in the middle of contact area. As a consequence, the vertical stiffness on the RuotaVia drum was found to be higher than that one on the flat track.
- The curvature of the RuotaVia drum mainly changes the length of contact patch, with a reduction from RuotaVia drum to flat track in the order of 10%. The area of contact tyre/rolling surface that is on average 12% reduced with respect to flat track.
- A correct inflation pressure is hard to recommend. Nowadays, manufacturers consider the static deflection or the feeling of the rider to define an optimal inflation pressure. The latter affects many parameters, so that a deeper study is necessary to define a standardized method useful to define the best inflation pressure.
- The stiffness of the rim largely affects the lateral characteristics of the tyre. It was found that the use of high-stiffness rim can ensure up to 13% higher cornering stiffness for tyres tested under the same working conditions.
- The study of the combined effect of inflation pressure and vertical load may be a good approach to suggest the best set-up for tyres; nonetheless a synthetic index useful for final user is still hard to find since the measurements strongly depend on other variables such as speed and temperature of the rolling surface.
- The effect of the speed on the lateral force does not affect so much the measurement of the lateral force F_y, nonetheless the increase of speed means higher energy to be dissipated to avoid the detrimental effect of the temperature.
- Temperature of the rolling surface can largely affect the measurements. Specifically, an increase of temperature of 40 °C causes a decrease of lateral force about 16%. This aspect may change bicycles dynamics, especially on paved roads featured by the presence of shaded corners during summer days.

In the future, it will be of great interest to test different type of bicycle tyres such as trekking or mountain bike tyres, featured by the presence of knobbles. The focus will be also devoted to the camber effect. Furthermore, a strong effort is required to provide synthetic indexes useful for final users to proper set tyre parameters.

Declaration of competing interest

The authors declare that they have no known competing financial interests or personal relationships that could have appeared to influence the work reported in this paper.

Data availability

Data will be made available on request.

Acknowledgements

The authors thank Lorenzo Uslenghi, Lorenzo Vaccari and Prof. Giorgio Previati for their support during the months of experimental test campaign.

References

Abràmoff, M.D., Magalhães, P.J., Ram, S.J., 2004. Image processing with imageJ. Biophot. Int. 11 (7), 36–41. https://doi.org/10.1201/9781420005615.ax4.
Berto, F., 2006. All about Tire Inflation.
Brooks, J.H.M., Tingay, R., Varney, J., 2021. Social distancing and COVID-19: an unprecedented active transport public health opportunity. BMJ Publishing Group Br. J. Sports Med. 55 (8), 411–412. https://doi.org/10.1136/bjsports-2020-102856. Apr. 01.
Bulsink, V.E., Doria, A., Van De Belt, D., Koopman, B., 2015. The effect of tyre and rider properties on the stability of a bicycle. Adv. Mech. Eng. 7 (12) https://doi.org/10.1177/1687814015622596. Dec.
Carahalios, A., 2015. An Analysis of the Bicycle-Rider Interface Forces in Stationary Road Cycling. University of Portland, 15275. July.
Corno, M., Panzani, G., Catenaro, E., Savaresi, S.M., 2021. Modeling and analysis of a bicycle equipped with in-wheel suspensions. Mech. Syst. Signal Process. 155 (Jun) https://doi.org/10.1016/j.ymssp.2020.107548.
Corwin, S., Zarif, R., Berdichevskiy, A., Pankratz, D., 2020. The futures of mobility after COVID-19. Scenarios for transportation in a postcoronavirus world. Deloitte Development LLC 1–21.

Dell'Orto, G., Mastinu, G., 2022. Effect of temperature on the mechanical characteristics of bicycle tyres. In: International Cycling Safety Conference 2022. Dresden.
Dell'Orto, G., Ballo, F.M., Mastinu, G., Gobbi, M., 2022a. Bicycle tyres – development of a new test-rig to measure mechanical characteristics. Measurement 202, 111813. https://doi.org/10.1016/J.MEASUREMENT.2022.111813. Oct.
Dell'Orto, G., Ballo, F.M., Mastinu, G., 2022b. Experimental methods to measure the lateral characteristics of bicycle tyres – a review. Veh. Syst. Dyn. 1–23. https://doi.org/10.1080/00423114.2022.2144388. Nov.
Deloitte's, T.M.T.. Technology, media, and Telecommunications Predictions 2020, 2020. [Online]. Available. https://www2.deloitte.com/content/dam/insights/us/articles/722835_tmt-predictions-2020/DI_TMT-Prediction-2020.pdf.
Doria, A., Roa Melo, S.D., 2018. On the influence of tyre and structural properties on the stability of bicycles. Veh. Syst. Dyn. 56 (6), 947–966. https://doi.org/10.1080/00423114.2017.1403032. Jun.
Doria, A., Tognazzo, M., Cusimano, G., Bulsink, V., Cooke, A., Koopman, B., 2013. Identification of the mechanical properties of bicycle tyres for modelling of bicycle dynamics. Veh. Syst. Dyn. 51 (3), 405–420. https://doi.org/10.1080/00423114.2012.754048. Mar.
Evangelou, S., 2003. The Control and Stability Analysis of Two – Wheeled Road Vehicles. no. September, p. 181. to the University of London for the degree of Doctor of [Online]. Available: http://www3.ic.ac.uk/pls/portallive/docs/1/50172.PDF.
Farroni, F., Giordano, D., Russo, M., Timpone, F., 2014. TRT: thermo racing tyre a physical model to predict the tyre temperature distribution. Meccanica 48 (3), 707–723. https://doi.org/10.1007/s11012-013-9821-9.
Farroni, F., Mancinelli, N., Timpone, F., 2020. A real-time thermal model for the analysis of tire/road interaction in motorcycle applications. Appl. Sci. 10 (5) https://doi.org/10.3390/app10051604.
Heine, J., 2006. Optimizing your tire pressure for your weight. Bicycle Quarterly 5 (4), 1–2.
Hess, R., Moore, J.K., Hubbard, M., 2012. Modeling the manually controlled bicycle. IEEE Trans. Syst. Man Cybern. Syst. Hum. 42 (3), 545–557. https://doi.org/10.1109/TSMCA.2011.2164244.
Klinger, F., Nusime, J., Edelmann, J., Plöchl, M., 2014. Wobble of a racing bicycle with a rider hands on and hands off the handlebar. Veh. Syst. Dyn. 52 (Suppl. 1), 51–68. https://doi.org/10.1080/00423114.2013.877592.
Kresie, S.W., Moore, J.K., Hubbard, M., Hess, R.A., 2017. Experimental validation of bicycle handling prediction. Davis, California, USA. In: 6th Annual International Cycling Safety Conference [Online]. Available: http://creativecommons.org/licenses/by/4.0/.1.
Maier, O., Hillenbrand, S., Wrede, J., Freund, A., Gauterin, F., 2018. Vertical and longitudinal characteristics of a bicycle tire. Tire Sci. Technol. 46 (3), 153–173.
Mastinu, G., Ploechl, M., 2014. Road and Off-Road Vehicle System Dynamics Handbook. Taylor & Francis Group, LLC.
Mastinu, G., Pennati, M., Gobbi, M., 2002. Design and construction of a test rig for assessing tyre characteristics at rollover. SAE Technical Papers. https://doi.org/10.4271/2002-01-2077 no. 724.
Moore, J.K., 2012. Human Control of a Bicycle. PhD Thesis. University of California [Online]. Available: http://moorepants.github.com/dissertation.
Pacejka, H.B., 2006. Tire and Vehicle Dynamics. https://doi.org/10.1016/B978-0-7506-6918-4.X5000-X.
Phromjan, J., Suvanjumrat, C., 2020. The contact patch analysis of solid tire on drum testing by finite element method. IOP Conf. Ser. Mater. Sci. Eng. 886 (1) https://doi.org/10.1088/1757-899X/886/1/012049.
SAE International, 2019. Surface Vehicle Information Report, pp. 1–96. J2047.
Schneider, C.A., Rasband, W.S., Eliceiri, K.W., 2012. NIH Image to ImageJ: 25 years of image analysis. Nat. Methods 9 (7), 671–675. https://doi.org/10.1038/nmeth.2089.
Sharp, R.S., 1971. The stability and Control of Motorcycles I (5), 316–329.
Sharp, R.S., 1993. Tyre Models for Vehicle Dynamics Analysis 21 (Suppl. L). https://doi.org/10.1115/1.2895925.
Swami, A., Liu, C., Kubenz, J., Prokop, G., Pandey, A.K., 2021. Experimental study on tire contact patch characteristics for vehicle handling with enhanced optical measuring system. SAE Int J Veh Dyn Stab NVH 5 (3). https://doi.org/10.4271/10-05-03-0023. Apr.
Takács, D., Orosz, G., Stépán, G., 2009. Delay effects in shimmy dynamics of wheels with stretched string-like tyres. Eur. J. Mech. Solid. 28 (3), 516–525. https://doi.org/10.1016/j.euromechsol.2008.11.007.
Tomiati, N., Magnani, G., Scaglioni, B., Ferretti, G., 2017. Model based analysis of shimmy in a racing bicycle. May 15-17, 2017. In: Proceedings of the 12th International Modelica Conference. Linköping University Electronic Press, Prague, Czech Republic, pp. 441–447. https://doi.org/10.3384/ecp17132441. Jul.
Tomiati, N., Colombo, A., Magnani, G., 2019. A nonlinear model of bicycle shimmy. Veh. Syst. Dyn. 57 (3), 315–335. https://doi.org/10.1080/00423114.2018.1465574. Mar.
Yang, Y., Wu, X., Zhou, P., Gou, Z., Lu, Y., 2019. Towards a cycling-friendly city: an updated review of the associations between built environment and cycling behaviors (2007–2017). J. Transport Health 14. https://doi.org/10.1016/j.jth.2019.100613. Sep.